JACS
JOURNAL OF THE AMERICAN CHEMICAL SOCIETY
Article
pubs.acs.org/JACS

A Molecular Tetrad That Generates a High-Energy Charge-Separated State by Mimicking the Photosynthetic Z-Scheme

Ludovic Favereau,[†] Abhinandan Makhal,[‡] Yann Pellegrin,[†] Errol Blart,[†] Jonas Petersson,[‡] Erik Göransson,[‡] Leif Hammarström,*[,‡] and Fabrice Odobel*[,†]

[†]CEISAM, Chimie et Interdisciplinarité, Synthèse, Analyse, Modélisation, CNRS, UMR CNRS 6230, Université de Nantes, 2 rue de la Houssinière, BP 92208, Nantes 44322 Cedex 3, France

[‡]Department of Chemistry—Ångström Laboratory, Uppsala University, Box 523, Uppsala, SE75120 Sweden

Supporting Information

ABSTRACT: The oxygenic photosynthesis of green plants, green algae, and cyanobacteria is the major provider of energy-rich compounds in the biosphere. The so-called "Z-scheme" is at the heart of this "engine of life". Two photosystems (photosystem I and II) work in series to build up a higher redox ability than each photosystem alone can provide, which is necessary to drive water oxidation into oxygen and $NADP^+$ reduction into NADPH with visible light. Here we show a mimic of the Z-scheme with a molecular tetrad. The tetrad Bodipy−NDI−TAPD−Ru is composed of two different dyes—4,4-difluoro-1,3,5,7-tetramethyl-2,6-diethyl-4-bora-3a,4a-diaza-*s*-indacene (Bodipy) and a $Ru^{II}(bipyridine)_3$ (Ru) derivative—which are connected to a naphthalene diimide (NDI) electron acceptor and tetraalkylphenyldiamine (TAPD) playing the role of electron donor. A strong laser pulse excitation of visible light where the two dye molecules (Ru and Bodipy) absorb with equal probability leads to the cooperative formation of a highly energetic charge-separated state composed of an oxidized Bodipy and a reduced Ru. The latter state cannot be reached by one single-photon absorption. The energy of the final charge-separated state (oxidized Bodipy/reduced Ru) in the tetrad lies higher than that in the reference dyads (Bodipy−NDI and TAPD−Ru), leading to the energy efficiency of the tetrad being 47% of the sum of the photon threshold energies. Its lifetime was increased by several orders of magnitude compared to that in the reference dyads Bodipy−NDI and TAPD−Ru, as it passes from about 3 ns in each dyad to 850 ns in the tetrad. The overall quantum yield formation of this extended charge-separated state is estimated to be 24%. Our proof-of-concept result demonstrates the capability to translate a crucial photosynthetic energy conversion principle into man-made molecular systems for solar fuel formation, to obtain products of higher energy content than those produced by a single photon absorption.

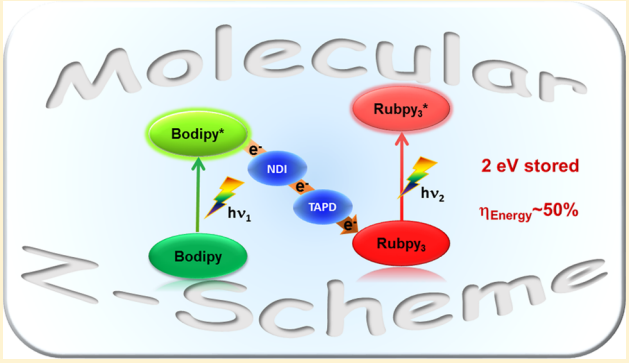

INTRODUCTION

The reaction centers of natural photosynthesis provide a blueprint for the design of molecular devices for the conversion of solar energy into fuels. This has inspired numerous efforts to mimic their working principles with the aim to develop our fundamental understanding as well as to explore possibilities for future renewable fuel technologies.[1] Oxygenic photosynthesis allows plants, green algae, and cyanobacteria to use water as their electron source to reduce CO_2 to carbohydrates. The possibility to use sunlight to activate cheap and stable raw materials such as water and CO_2 to form carbon-based fuels is a particularly attractive concept. This chemistry requires generation of both a strong oxidant to split water and a strong reductant to form NADPH that is used for CO_2 reduction. This is achieved by photosystems I and II (PSI and PSII), which accomplish five distinct tasks in concert to store solar energy in the form of chemical bonds: (1) light harvesting; (2) transformation of the photon energy into a long-lived charge-separated state; (3) accumulation of several redox equivalents upon consecutive absorption of several photons; (4) redox wiring of PSI to PSII to yield both a strong reductant (in PSI) and a strong oxidant (in PSII); this also leads to a transmembrane proton gradient which activates the ATP synthase; and, finally, (5) coupling of the high-energy charge-separated state to the catalytic systems ferredoxine NADP reductase (FNR) in PSI and oxygen-evolving complex (OEC) in PSII, which respectively reduce $NADP^+$ into NADPH and oxidize water into oxygen (Figure 1).

The two first functions of this multifunctional molecular machinery are relatively well-mastered in artificial multicomponent molecular arrays, since there are elegant architectures mimicking the light-harvesting antenna[2] or transforming sunlight into a long-lived charge-separated state with a high quantum yield.[3] There are also a few examples of systems featuring photoinduced accumulative charge separation

Received: December 3, 2015
Published: February 29, 2016

DOI: 10.1021/jacs.5b12650
J. Am. Chem. Soc. 2016, 138, 3752−3760

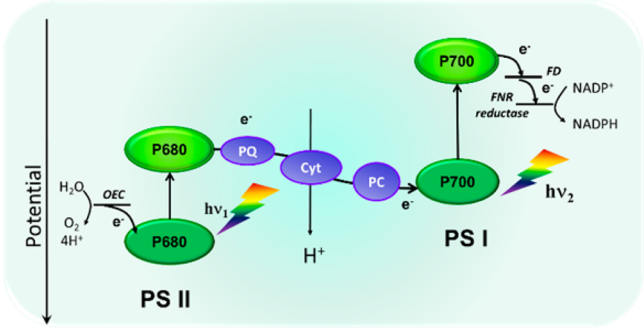

Figure 1. Schematic illustration of the Z-scheme function in green plants. OEC = oxygen-evolving complex; PQ = plastoquinone pool; Cyt = cytochrome; PC = plastocyanin; FD = ferredoxin; FNR = ferredoxin $NADP^+$ reductase.

of multiple electron–hole pairs without the use of sacrificial agents.[4] The development of photocatalytic systems generating fuels with sunlight started by the end of 1970s,[5] and there are many systems combining sensitizers and molecular catalysts that evolve hydrogen[6] or CO from CO_2[7] upon visible light irradiation.

However, despite these major advances, practical, cost-effective technologies for large-scale and environmentally friendly conversion of sunlight into solar fuels still remain a considerable challenge to achieve. One of the main reasons for that is the difficulty to combine all these biomimetic tasks together to perform a complete photosynthetic process as nature does with the oxygenic photosynthesis. For instance, the strategy used so far to optimize photocatalytic systems is to divide the overall process into its two half-reactions (H_2 photoproduction and O_2 formation), where a sacrificial agent provides the complementary reductive or oxidative equivalents. However, practical, cost-effective technologies for large-scale and environmentally friendly conversion of sunlight into fuels cannot consume high-energy sacrificial reagents. Instead, connecting the two photocatalytic systems without sacrificial agent is now the major challenge of artificial photosynthesis. One obstacle to overcome is the difficulty of generating both a strongly reducing and strongly oxidizing charge-separated state by absorption of a single photon of visible light. Accordingly, it is necessary to explore new concepts to solve the aforementioned problem.

Green plants take up this challenge thanks to the Z-scheme function, which relies on the connection in series of two photosystems (PSI and PSII), both independently realizing the conversion of a photon into a charge-separated state.[8] In PSII, the absorption of a first photon promotes the oxidation of the central chlorophyll pigments (P680) and the reduction of a quinone (Q). Another light absorption in PSI leads to the photo-oxidation of P700 and a reduced ferredoxin (FD) (Figure 1). An electron transport chain composed of mobile electron transporters conveys the electron on the reduced quinone to the oxidized $P700^+$. Overall, the electrons removed from water in PSII are activated by two photons from sunlight in two different photosystems to reach a sufficient potential enabling the reduction of $NADP^+$ into NADPH. Conceptually, the energy produced in PSII is partly injected into PSI. As a result, a large difference of potentials can be reached between the final oxidant ($P680^+$; $E \approx 1.4$ V vs SCE)[9] and the final reductant (FD^-; $E \approx -1$ V vs SCE)[9] thanks to the buildup of a potential created by two photons absorbed in two different photosystems. This ingenious strategy outlines a path toward efficient artificial photosynthetic systems.

Despite its major involvement in the oxygenic photosynthesis, Z-scheme artificial systems involving two-step photoexcitation under visible light irradiation are rare and the vast majority of them rely on two inorganic semiconductors (SCs) exchanging charges with a redox couple[10] or bound together via a metal junction.[11] To the best of the authors' knowledge, there are only two reports of a Z-scheme mimic with molecular systems. One is not entirely molecular but is a molecular dyad grafted on a low band gap SC,[12] which photocatalytically reduced CO_2 into formic acid while at the same time oxidizing methanol; methanol is a high-energy sacrificial donor, as opposed to water, which is a low-energy sacrificial donor. The second example is a "molecular AND gate" with two linked chromophore-donor dyads that operated on the basis of a Z-scheme charge separation; however, the purpose was not to increase the charge separation energy, as the resulting state had lower energy (1.14 eV) than each of the charge-separated states generated by single excitation.[13] In a molecular Z-scheme, each separated electron–hole pair should be energized by two photons. This is different from photoaccumulation of several electron–hole pairs[4b] or photoaccumulation of redox equivalents with sacrificial reagents.[6a,14] The advantages of a Z-

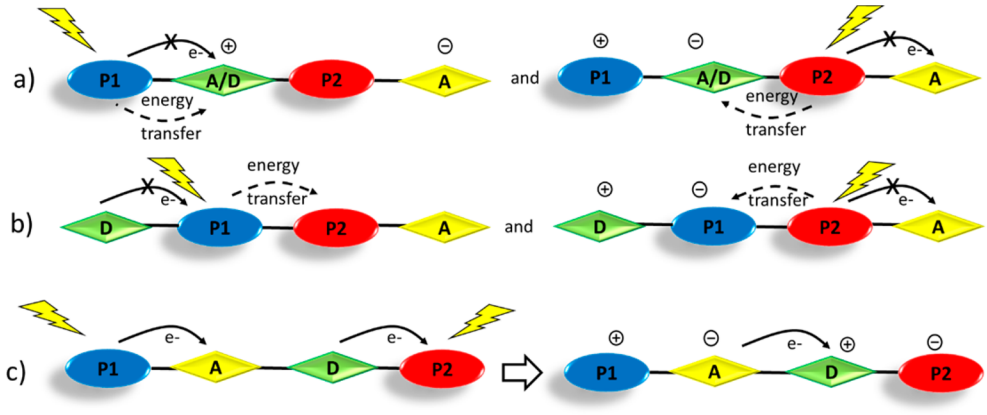

Figure 2. Illustration of three possible molecular organizations of the components to build a Z-scheme tetrad and their respective critical reaction intermediates, as discussed in the text (dashed arrows show some important counterproductive side reactions but not an exhaustive list). P1 and P2 = photosensitizers; A = electron acceptor; D = electron donor.

DOI: 10.1021/jacs.5b12650
J. Am. Chem. Soc. 2016, 138, 3752–3760

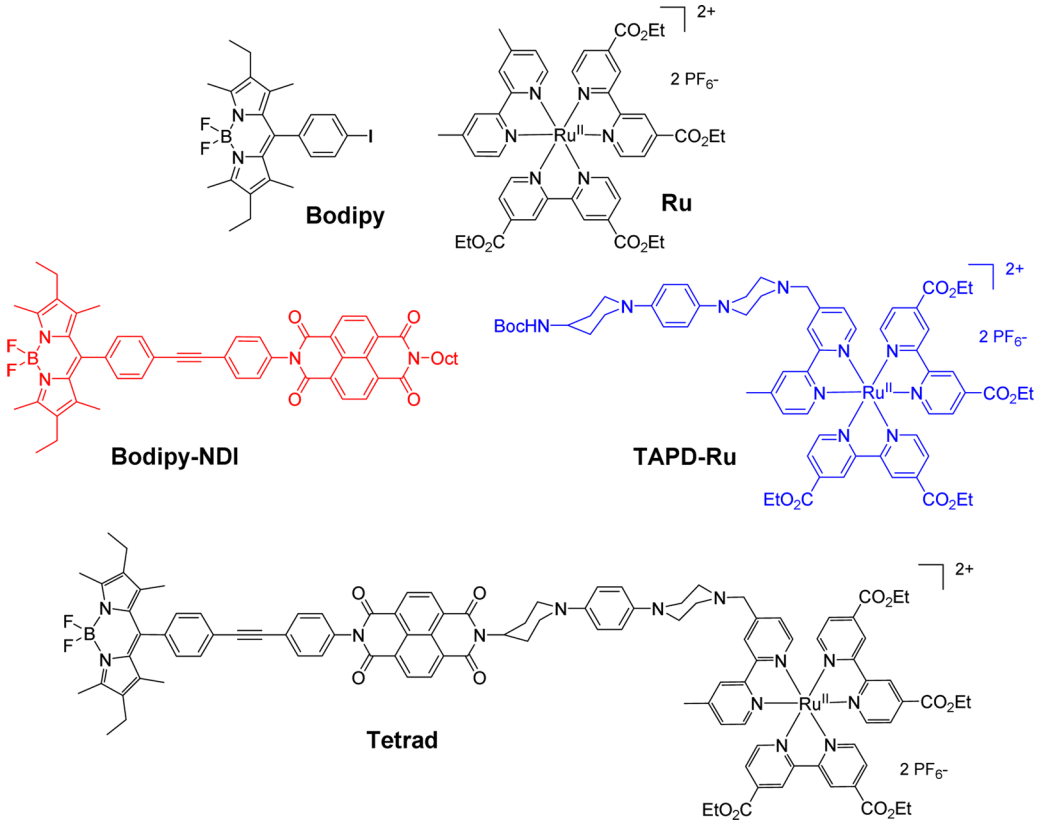

Figure 3. Molecular structures of the tetrad and its reference building blocks.

scheme approach compared to a single visible-light-responsive photosystem stems from the possibility to exploit a wider range of the solar spectrum, because the photonic energy required to build up the oxidant and the reductant in each photosystem can be reduced [Figure S12, Supporting Information (SI)]. Indeed, because of entropic and overpotential losses required to drive catalysis at appreciable rates, an artificial water-splitting system needs significantly more excitation energy than what is required for water splitting under standard conditions (1.23 eV), probably at least around 1.8 V.[15] In contrast, long-lived molecular charge separation in tetrads, pentads, etc., built on single excitation have at best stored ca. 1.1 eV in their final charge-separated state.[3a−d] Considering the unique advantage of the Z-scheme principle, we have decided to construct a molecular Z-scheme mimic driven by two-step photoexcitation in two different artificial photosystems (Figure 2). For this purpose, we designed the tetrad molecule Bodipy−NDI−TAPD−Ru (Figure 3), composed of two different dyes—the organic dye 4,4-difluoro-1,3,5,7-tetramethyl-2,6-diethyl-4-bora-3a,4a-diaza-*s*-indacene (Bodipy) and a Ru^{II}(bipyridine)$_3$ derivative which harvest light in a complementary manner between 400 and 600 nm. The naphthalene diimide (NDI)[16] unit is a good electron acceptor, while the tetraalkylphenyldiamine (TAPD) unit is a good electron donor.[17] The ultimate charge-separated state produced by two-photon excitation is where Bodipy is oxidized and Ru is reduced. We report herein the unique property of a molecular tetrad in which two coupled photoinduced electron transfer events derived from two consecutive photon absorptions produce a long-lived charge-separated state composed of both a strong oxidant and reductant (Figure 7). Its photochemical behavior relies on the Z-scheme operation principle (Figure 1). This tetrad constitutes a rare example of a molecular model capable of multiple electron redox events deriving from a defined molecular architecture, thus mimicking the natural Z-scheme principle found in oxygenic photosynthesis.

MOLECULAR DESIGN OF AN ARTIFICIAL Z-SCHEME SYSTEM

The design has followed a number of careful considerations (Figure 2). First, the dye absorption spectra must allow for both selective single excitation and simultaneous excitation of the two dyes. Second, the final charge separation state must be possible to distinguish by transient optical spectroscopy from the states formed by single excitation of either dye. Third, the energy of the final charge-separated state should be high, so that the ultimate donor is oxidized at a high potential and the ultimate acceptor is reduced at a low potential. The fourth point of consideration is an important part of the successful design, where we decided on a conceptually novel use of a controlled recombination between intermediate radicals to reach the ultimate charge separation. The rationale is less obvious and requires more careful elaboration. Excited states of dyes can react via several pathways, in addition to the desired electron transfer.[4c,d] The excited dye is often both a good oxidant and reductant, which may lead to electron transfer in the wrong direction. For example, while the reduced plastocyanine in oxygenic photosynthesis delivers electrons to photosystem I, plastocyanine in its oxidized form is thermodynamically quite able to, instead, accept an electron from the excited P_{700} chlorophylls, were it allowed to interact directly. In addition, radical intermediates can often be quenched by energy transfer or paramagnetic interaction. These reactions compete with the desired charge separation

DOI: 10.1021/jacs.5b12650
J. Am. Chem. Soc. 2016, 138, 3752−3760

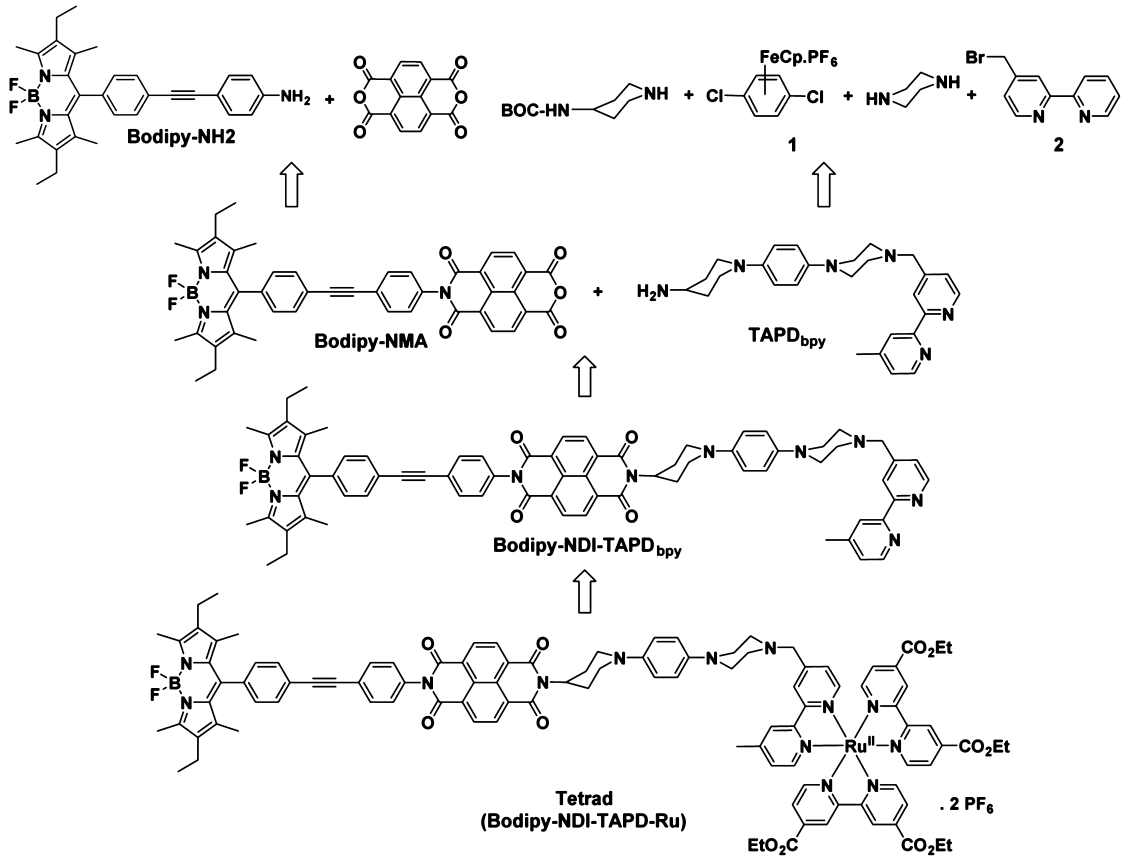

Figure 4. Retrosynthetic strategy for the tetrad (Bodipy−NDI−TAPD−Ru).

and may be a problem when using a more intuitive design topology of a Z-scheme tetrad (Figure 2). For these reasons, we designed our tetrad so that the radical products of each dye excitation do not come in direct contact with the other dye (Figure 2c). There are, basically, three strategies to assemble the components to build the tetrad (Figure 2). First, an intuitive linear charge separation design corresponds to the assembly of two dyads, P_1−A/D and P_2−A, to one another (Figure 2a). Let us imagine that the first photon has successfully created the expected charge-separated state via excitation of the photosensitizer [P2 (left panel) or P1 (right panel) in Figure 2a]. However, first the intermediate unit A/D must be able to be both an electron donor and acceptor, depending on which photosensitizer is excited first. This requires two successive redox potentials in the span between the $P1^{+/*0}$ and $P2^{*0/-}$ potentials. Second, the excited state of the second photoexcited dye will sit next to a radical (D^+ in the left case, A^- in the right case), which increases the risk of unproductive quenching reactions by energy or reverse electron transfer. An alternative strategy is the case where P1 and P2 are directly connected next to each other and are located at the center of the system (Figure 2b). The drawbacks are, first, that the higher-lying photosensitizer excited state (here P1 in Figure 2b) may systematically be quenched by energy transfer by the nearby dye with the lower-lying excited state, precluding thus the charge transfer reaction in one photosystem (left panel in Figure 2b) and, second, that even if the first excitation on P1 leads to charge separation, the second excited dye may be quenched by the adjacent radical ($P1^-$) rather than by A (right panel in Figure 2b). The third organization (Figure 2c), in which the photosensitizers (P1 and P2) are placed at the extremities of the molecule, is an unusual strategy, but it is here shown to be successful for the Z-scheme operation principle. The photosensitizers P1 and P2 each react independently with their respective donor/acceptor (A and D; left panel). The intermediate state A^-/D^+ undergoes rapid charge recombination (charge collapse) to stabilize the ultimate $P1^+$ $P2^-$ state (right panel). The intermediate (A^- or D^+) never sits near a sensitizer excited state. Consequently, the P_1−A−D−P_2 organization (Figure 2c) was chosen to assemble the components of the tetrad prepared and studied. In this work. P1 is Bodipy and P2 is a ruthenium tris(bipyridine) complex, as these dyes fulfill the requirements to give respectively a strong oxidant and a strong reductant after photoinduced electron transfer to the neighboring unit. The NDI unit is the electron acceptor, while the TAPD unit is the electron donor.

■ EXPERIMENTAL SECTION

The preparation and the characterizations of the compounds are described in the Supporting Information.

Transient Absorption Spectroscopy. All photophysical data were obtained in purified dichloromethane solvent, except for the TAPD−Ru dyad, which was investigated in CH_3CN for solubility reasons (selective femtosecond excitation of the tetrad in DCM showed that the results from single Ru-dye excitation were within experimental uncertainty identical in the two solvents). Femtosecond transient absorption experiments used amplified pulses (1 kHz, λ = 800 nm, fwhm 100 fs) that were split into a pump and a probe part. An optical parametric amplifier (TOPAS, Light Conversion) was used to generate the desired pump wavelength, with an energy of 300−500 nJ/pulse at the sample. The white light continuum probe was obtained by focusing part of the 800 nm light on a moving CaF_2 plate. Polarization of the pump was set at the magic angle, 54.7°, relative to the probe.

DOI: 10.1021/jacs.5b12650
J. Am. Chem. Soc. 2016, 138, 3752−3760

The instrumental response time was typically about 100 fs. The sample was contained in a 1 mm path length quartz cell that was moved horizontally during the experiment to prevent sample degradation. Each time scan used ca. 1000 accepted pulses per delay line position. Successive time scans (5−10) on each sample were recorded separately and compared to verify that no sample degradation occurred during data acquisition. Transient absorption data were processed using Origin 9 software. Transient absorption data were processed using Igor Pro 6.35A or Origin 9.0 software. All the femtosecond spectra are chirp-corrected. As the processes are very slow compared to the instrumental response (<200 fs), kinetic traces could be simply fitted by a nonlinear least-squares method using a single- or double-exponential decay function, without considering the response function or early time artifacts. More details are given in the Supporting Information.

For nanosecond transient absorption and photoemission measurements, a Q-switched Nd:YAG laser (Quanta-Ray ProSeries, Spectra-Physics) and an OPO were used to produced laser pulses at the desired wavelength with a fwhm of 15 ns. Probe light was provided at a right angle with respect to the pump light by a pulsed XBO 450 W xenon arc lamp (Osram). Transient spectra were recorded by the iStar CCD camera (Andor Technology) of an LP920-S laser flash photolysis spectrometer setup (Edinburgh Instruments) using the L900 software and processed using Origin 9 software. Transient traces at single wavelength were recorded with a LP920-K PMT detector, which was connected to a Tektronix TDS 3052 500 MHz 5 GS/s oscilloscope. These were fitted with a nonlinear least-squares method using a single-exponential decay function. A fluorescence quartz cell cuvette (Starna) with a 10 mm path length was used for measurements, and the samples were deoxygenated by purging with a gentle stream of argon for 10 min. With strong laser pulses (15 mJ/pulse and above) each transient spectrum or kinetic trace used was the first pulse given to a fresh sample to guarantee that data were unaffected by sample degradation.

RESULTS AND DISCUSSION

Synthesis. The structure of the tetrad and its corresponding components Bodipy−NDI and TAPD−Ru are shown in Figure 3. The synthesis and characterization of all these compounds are described in detail in the Supporting Information. From a retrosynthetic point of view, the ruthenium complex (photosensitizer P2) was prepared in the last step to avoid potential hydrolysis of the ester groups on the bipyridine ligands during the synthesis of the other subunits and to limit the number of purifications of charged molecules (Figure 4).

The two key building blocks Bodipy−NMA and $TAPD_{bpy}$ were prepared independently and also used for the preparation of reference compounds (see SI). Bodipy−NMA results from the condensation of Bodipy-NH_2 with naphthalene bis anhydride acid; the former was prepared from Sonogashira cross-coupling reaction between iodo-Bodipy and ethynylaniline. $TAPD_{bpy}$ was easily synthesized from the nucleophilic aromatic substitution of *p*-dichlorobenzene(cyclopentadienyl) iron (**1**) with piperazine derivatives followed by a final nucleophilic substitution with (bromomethyl)bipyridine (**2**).

Electronic Absorption Spectra and Electrochemistry. The absorption of the tetrad and the two corresponding dyads Bodipy−NDI and TAPD−Ru are given in Figure 5, and the spectroscopic data are collected in Table S1 (SI). The two sensitizers in the photosystems, Bodipy−NDI and TAPD−Ru, display distinct absorption bands that allow for quite selective excitation by using suitable wavelength. For example, in the tetrad the Bodipy can be photoexcited with >85% selectivity at 530 nm, while the ruthenium tris(bipyridine) complex can be addressed with >85% selectivity at 440 nm. Interestingly, at 490 nm both sensitizers have equal extinction coefficients and will be excited with equal probability. The redox potentials of the

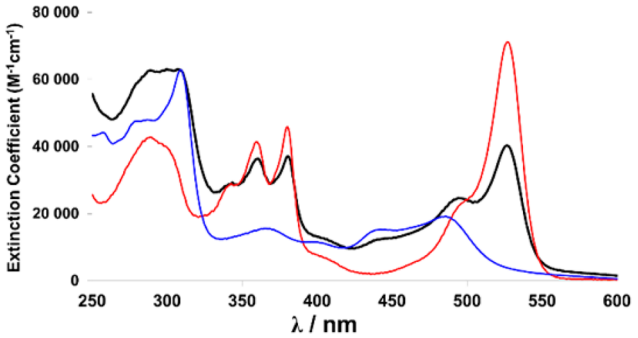

Figure 5. Absorption spectra of the tetrad (black) and the dyads Bodipy−NDI (red) and TAPD−Ru (blue). The spectra of the tetrad and TAPD−Ru are recorded in acetonitrile and that of Bodipy−NDI in dichloromethane (298 K).

tetrad and the dyads Bodipy−NDI and TAPD−Ru were measured by cyclic and square wave voltammetry and are all referenced versus a saturated calomel electrode (SCE) (Table S3, SI). The attribution of each process can be confidently made according to the redox potential of each subunit recorded independently, and they are in agreement with those reported for similar compounds (Table S3, SI). Overall, the comparison of the absorption and redox characteristics of the individual units with those in the dyads and in the tetrad evidence a weak electronic interaction between them. This conclusion is consistent with the attachment of the ruthenium complex to the TAPD and to NDI via nonconjugated linkers and with the existence of nodes in the LUMO and HOMO orbitals on the nitrogens of diimide groups of NDI. We note, however, that the transition on the Bodipy is weaker in the tetrad; a phenomenon that was already observed in previously published systems containing Bodipy and coordination complexes.[18]

In the tetrad, the first and second oxidation process is localized on the TAPD unit at 0.30 and 0.73 V, respectively, and then the Bodipy unit is oxidized at 1.05 V. Finally, a metal-centered oxidation occurs on the ruthenium complex at 1.51 V. In the cathodic region, the first wave corresponds to the reduction of the NDI at −0.59 V and then to a ligand-centered reduction on the diethyl bipyridine dicarboxylic ester of the ruthenium complex at −0.97 V.

The excited-state energy level derived from emission spectra and the redox potential values enable one to calculate the photoinduced electron transfer driving forces in each dyad with the Rehm−Weller formalism (Supporting Information). A diagram illustrates that all desired electron transfer processes are exergonic by at least −0.6 eV (Figure 7).

Photophysical Study by Transient Absorption Spectroscopy. Transient absorption spectroscopy experiments were undertaken to unravel the deactivation processes occurring in these dyads. The photoemission from the excited state of Bodipy and of the ruthenium complex in the parent dyads Bodipy−NDI and TAPD−Ru are quenched compared to the reference sensitizers by ca. 70% and 99%, respectively, in dichloromethane (Table S3, SI).

Excitation of the Bodipy reference at 530 nm with a 120 fs laser pulse forms the lowest excited S_1 state that shows a strong bleach of the ground-state absorption around 530 nm, together with stimulated emission in the red part of that region, and an absorption band around 430 nm (Figure S3, SI). These features disappear with a lifetime of 5.0 ns as the S_1 state converts to the ground state. In Bodipy−NDI, instead, the excited Bodipy leads

DOI: 10.1021/jacs.5b12650
J. Am. Chem. Soc. 2016, 138, 3752−3760

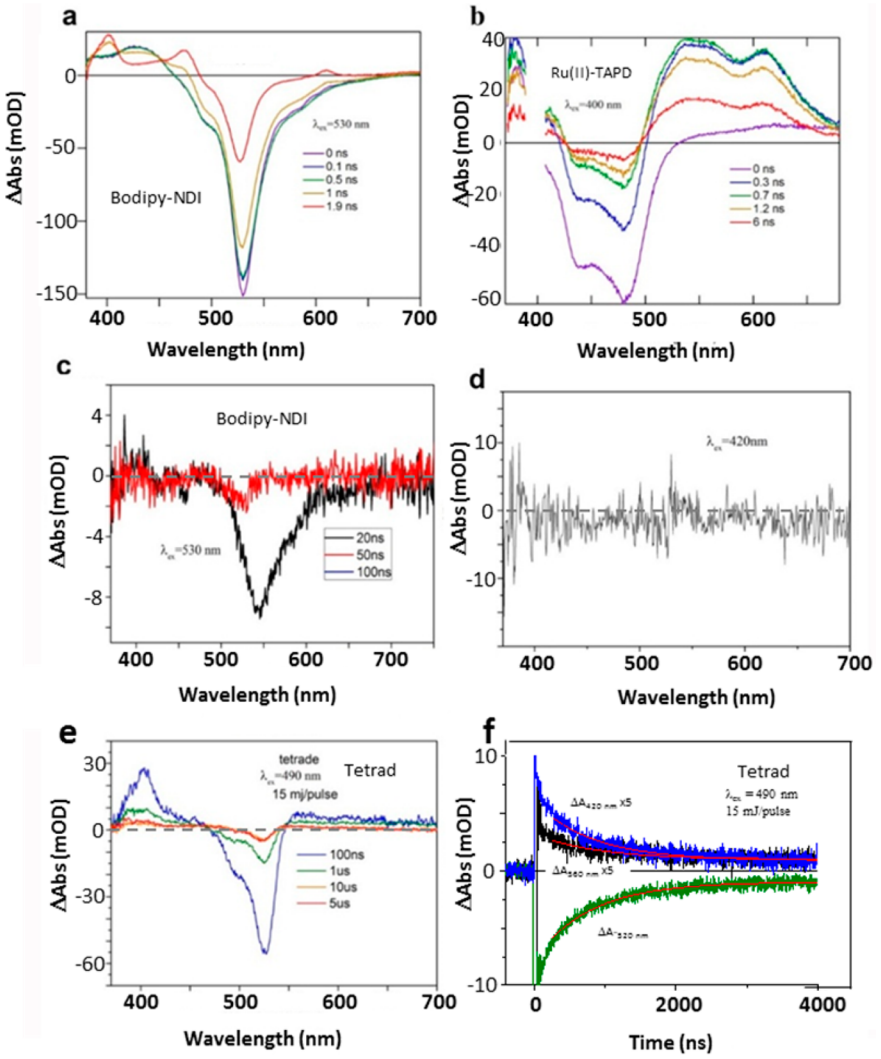

Figure 6. Transient absorption data. (a) Excitation with a 100 fs pulse of Bodipy−NDI at 530 nm generates the initial Bodipy excited state that converts to a charge-separated state with characteristic absorption at 400 nm ($Bodipy^+$) and 480 and 605 nm (NDI^-) as well as Bodipy ground-state bleach. (b) Excitation with a 100 fs pulse of Ru−TAPD at 400 nm generates the Ru^{2+} excited state that converts to a charge-separated state with characteristic absorption at 530 nm (Ru^+) and 610 nm ($TAPD^+$) as well as Ru^{2+} ground-state bleach. (c and d) Excitation with a 15 ns, 15 mJ pulse of only the Bodipy unit in Bodipy−NDI at 530 nm (panel c) or the Ru dye in the tetrad at 420 nm (panel d); the charge-separated state obtained after single excitation of each dye decays within 20 ns (cf. Figures S5 and S7, SI). See the text. (e) Excitation of the tetrad with a 15 ns, 15 mJ pulse at 490 nm that excites both dyes and leads to a long-lived (825 ns) charge-separated state with characteristic absorption at 400 nm ($Bodipy^+$ and some Ru^+) and a net absorption at 560 nm (Ru^+ minus Bodipy bleach) as well as ground-state bleach of both Bodipy (530 nm) and Ru^{2+} (480 nm). Note that no absorption is seen from either NDI^- or $TAPD^+$. (f) Transient absorption decay traces at significant wavelengths [420 nm (blue), 520 (green) and 560 nm (black)], corresponding to the experiment in panel e, showing intramolecular recombination of the $Bodipy^+$−Ru^+ state of the tetrad. The 420 and 560 nm traces are multiplied by a factor of 5 to facilitate comparison. The red lines are single exponential fits to the individual traces with $\tau = 0.85 \pm 0.1$ μs.

to the formation of the $Bodipy^+$−NDI^- charge-separated state with τ_{obs} = 0.9 ns, as seen by the formation of Bodipy absorption at 400 nm and characteristic NDI^- absorption bands at 475 and 605 nm (Figure 6a). The charge-separated state then recombines to the ground state with τ_{CR} = 3.0 ns (Figure S5, SI).

Excitation of the Ru unit in TAPD−Ru at 400 nm resulted in quenching of the lowest ^{3}MLCT state by formation of the $TAPD^+$−Ru^- charge-separated state with τ_{obs} = 1.1 ns, as seen by the formation of characteristic bands of reduced Ru at 380 and 530 nm and of $TAPD^+$ at 610 nm (Figure 6b). For comparison, the ^{3}MLCT lifetime in the Ru reference complex is much more long-lived, 500 ns (Figure S6, SI). The $TAPD^+$−Ru^- state formed in the dyad then recombines with τ_{CR} = 3.5 ns (Figure S7, SI).

Selective excitation of the tetrad with a 120 fs pulse at either 440 or 530 nm gave results that were the same as for excitation of the respective dyad, consistent with a weak interaction between the subunits (Figures S8 and S9, SI).

The ca. 3 ns lifetime of the charge-separated state of each subunit allowed us to achieve double excitation of a large fraction of the tetrad sample by using a strong 15 ns laser pulse at 490 nm. In this way we should generate both the $Bodipy^+$−NDI^- and $TAPD^+$−Ru^- states in the same tetrad within the same pulse upon absorption of one photon by Ru and another by Bodipy. The results of the transient absorption study are shown in Figure 6e,f. Interestingly, this experiment resulted in

DOI: 10.1021/jacs.5b12650
J. Am. Chem. Soc. 2016, 138, 3752−3760

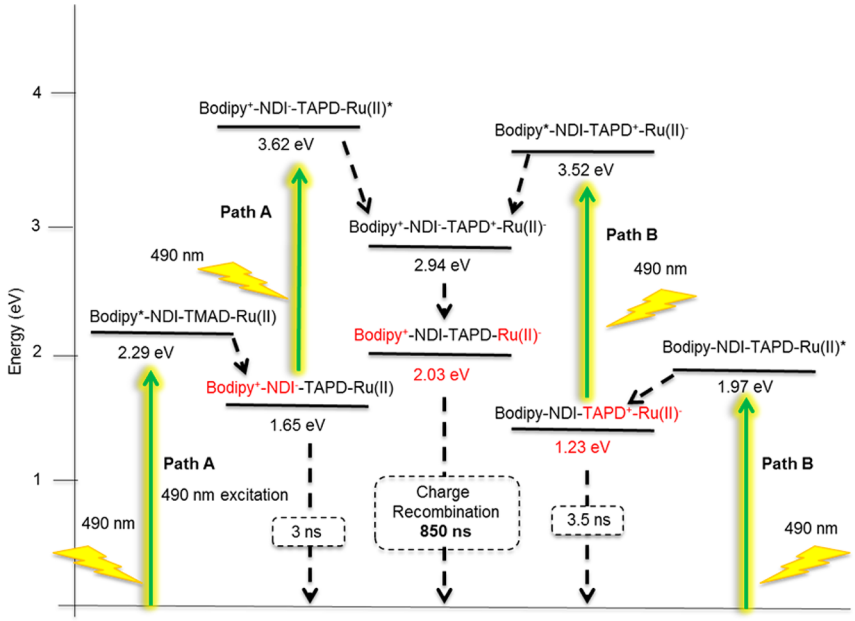

Figure 7. Schematic energy diagram showing the pertinent states involves in the deactivation of the tetrad via the Z-scheme principle.

formation of a much more long-lived state, one that shows the features of both Bodipy$^+$ (400 nm absorption, 530 nm bleach) and Ru$^-$ (380 and 550 nm absorption, 480 nm bleach) but with no sign of TAPD$^+$ or NDI$^-$. The high extinction coefficients for the Bodipy species dominate, but the presence of Ru$^-$ is clear from the positive absorption around 550 nm, where the Bodipy−NDI dyad and Bodipy excited state instead show a net bleach (cf. Figures 6a and S3, SI), and the additional 480 nm bleach. The relative signal magnitudes at 530 and 560 nm agree well with a 1:1 (±20%) formation of Bodipy$^+$ and Ru$^-$ and the species extinction coefficients (see SI and Figures S3 and S4 for details). Importantly, all these features decay with the same lifetime of τ_{CR} = 0.85 ± 0.1 μs (Figure 6f), which gives evidence for formation of an intramolecular charge-separated state Bodipy$^+$−NDI−TAPD−Ru$^-$ that recombines in a 1:1 fashion. The slight deviation from single-exponential kinetics is similar for all wavelengths and may be attributed to the conformational flexibility of the tetrad. Note that at the low product concentrations produced in flash photolysis (<10 μM) bimolecular recombination can be excluded on the time scale of 0.85 μs. Control experiments were performed by exciting Bodipy−NDI at 490 nm or the tetrad at 440 nm (where only the Ru unit absorbs) and resulted in no detectable signal on the time scale of >50 ns (Figure 6c,d).[19] This shows that excitation of both dyes in the tetrad are needed to form the long-lived Bodipy$^+$−NDI−TAPD−Ru$^-$ state observed. This result can be explained by an efficient charge collapse of the Bodipy$^+$−NDI$^-$−TAPD$^+$−Ru$^-$ state, which is generated by excitation of both dyes, to form the Bodipy$^+$−NDI−TAPD−Ru$^-$ before the ca. 3 ns recombination occurs within the individual photosystems Bodipy$^+$−NDI$^-$ and TAPD$^+$−Ru$^-$ (see Figure 7). An estimate of the quantum yield of Bodipy$^+$−NDI−TAPD−Ru$^-$ formation was made from the maximum Bodipy bleach at 530 nm in the tetrad and compared to a theoretical maximum value, and this comparison indicated that the charge collapse with 15 mJ pulses is near quantitative, i.e., $\tau_{collapse} \ll 3$ ns (see Supporting Information). The charge separation yield is within experimental uncertainty equal to the theoretical maximum of 24%; the maximum is limited by the fact that charge separation takes a finite time and the laser pulse is broad, so that one local charge-separated state may decay before the second one is formed (see the SI for details). The excitation power dependence of the transient signal amplitudes could not distinguish the expected quadratic dependence from a trivial linear dependence, because compound degradation at higher powers caused an even less than linear increase and, eventually, even a decrease in signal (Figure S10, SI) The design of the tetrad was successful in allowing for generation of a high-energy and long-lived charge-separated state via the Z-scheme. Note that we could not study the collapse process directly, even if we would use 120 fs pulses, because formation of each initial charge-separated state occurs with $\tau_{obs} \approx 1$ ns, which is much slower than the subsequent collapse.

The energy stored in the charge-separated state formed in the dyad Bodipy−NDI corresponds to 1.65 eV, while that in TAPD−Ru is 1.23 eV (Figure 7 and Supporting Information). In the tetrad the two stepwise photon absorptions lead to the formation of a unique charge-separated state storing the energy content of 2.03 eV (Figure 7). The energy introduced into the system in the form of light with two photons (2.29 + 1.97 = 4.26 eV) is finally stored in a high-lying charge-separated state (2.03 eV) in the form of a strong oxidant (Bodipy$^+$ E_{OX} = 1.05 V) and a strong reductant [Ru(I) E_{Red} v= −0.97 V]. The energy efficiency of the tetrad is therefore 47% of the sum of the photon threshold energies. In addition, the lifetime of the final charge-separated state has been increased by several orders of magnitude as it passes from about 3 ns in each dyad Bodipy−NDI and TAPD−Ru to 850 ns in the tetrad. This example clearly highlights the advantage of developing artificial Z-scheme systems that can generate a high-energy and long-lived charge-separated state with two photons from visible light.

■ CONCLUSIONS

This study has demonstrated a successful mimic of the Z-scheme principle found in oxygenic photosynthesis within an artificial molecular system in which two charge separation events deriving from two distinct excitations can take place within two linked photosystems. The latter system was inspired

DOI: 10.1021/jacs.5b12650
J. Am. Chem. Soc. 2016, 138, 3752−3760

by natural photosynthesis in green plants and is called the Z-scheme. This system is unique as it ultimately leads to a single charge-separated state, which stores a larger energy content than the individual photosystems do and provides thus the possibility to generate both a strong oxidant and a strong reductant with two photons of the visible spectrum. As such, the Z-scheme principle represents a valuable strategy to implement in photomolecular catalysts in order to drive energy-demanding redox transformations. The presented molecular design, while respecting the sequence of P_1/A/D/P_2, represents a guideline to synthesize supramolecular or hybrid systems that can be easier to prepare and to be used to exploit the high-energy photodriven charge-separated state. Currently, the necessity to photoexcite the system with a strong laser pulse to initiate two charge separation events represents the major limitation for the practical use of the tetrad in the present form. This means that another function must be introduced to amplify the sun fluence. This feature exists in photosynthetic organisms, which are equipped with light-harvesting antennas. The role of the latter is to increase the frequency at which the same chromophores is photoexcited to perform multiple turnovers under the low-light conditions of terrestrial sun irradiation. Accordingly, a light-harvesting antenna is a supplementary function that is ultimately required to perform charge photoaccumulation or Z-scheme function under sun fluence with molecular systems. However, the demonstration within a well-characterized model establishes a first link between fundamental studies of biological electron transfer and application for solar fuel production.

■ ASSOCIATED CONTENT

Supporting Information

The Supporting Information is available free of charge on the ACS Publications website at DOI: 10.1021/jacs.5b12650.

Description of the detailed synthetic procedures, electronic absorption and emission properties, electrochemical properties, spectroelectrochemistry, additional transient absorption and photoemission experiments, and NMR spectra of new compounds (PDF)

■ AUTHOR INFORMATION

Corresponding Authors

*Leif.Hammarstrom@kemi.uu.se

*Fabrice.Odobel@univ-nantes.fr

Notes

The authors declare no competing financial interests.

■ ACKNOWLEDGMENTS

We thank the Agence Nationale de Recherche (ANR) for the financial support through the ANR Blanc "MolecularZScheme" (ANR-13-BS07-0016-01). A.M., E.G, J.P., and L.H. are grateful for support from the Knut and Alice Wallenberg Foundation and the Swedish Energy Agency. Région Pays de la Loire for LUMOMAT project and COST Action (CM1202 PERSPECT-H2O) are also acknowledged for support of this work.

■ REFERENCES

(1) (a) Lewis, N. S.; Nocera, D. G. *Proc. Natl. Acad. Sci. U. S. A.* **2006**, *103*, 15729−15735. (b) LaVan, D. A.; Cha, J. N. *Proc. Natl. Acad. Sci. U. S. A.* **2006**, *103*, 5251−5255. (c) Hambourger, M.; Moore, G. F.; Kramer, D. M.; Gust, D.; Moore, A. L.; Moore, T. A. *Chem. Soc. Rev.* **2009**, *38*, 25−35.

(2) (a) Adronov, A.; Frechet, J. M. J. *Chem. Commun.* **2000**, 1701−1710. (b) Choi, M.-S.; Yamazaki, T.; Yamazaki, I.; Aida, T. *Angew. Chem., Int. Ed.* **2004**, *43*, 150−158. (c) Nakano, A.; Osuka, A.; Yamazaki, T.; Nishimura, Y.; Akimoto, S.; Yamazaki, I.; Itaya, A.; Murakami, M.; Miyasaka, H. *Chem. - Eur. J.* **2001**, *7*, 3134−3151. (d) Aratani, N.; Kim, D.; Osuka, A. *Acc. Chem. Res.* **2009**, *42*, 1922−1934. (e) Balzani, V.; Campagna, S.; Denti, G.; Juris, A.; Serroni, S.; Venturi, M. *Acc. Chem. Res.* **1998**, *31*, 26−34. (f) Zhou, X.; Tyson, D. S.; Castellano, F. N. *Angew. Chem., Int. Ed.* **2000**, *39*, 4301−4305.

(3) (a) Gust, D.; Moore, T. A.; Moore, A. L.; Lee, S. J.; Bittersmann, E.; Luttrull, D. K.; Rehms, A. A.; DeGraziano, J. M.; Ma, X. C.; Gao, F.; Belford, R. E.; Trier, T. T. *Science* **1990**, *248*, 199−201. (b) Balzani, V.; Credi, A.; Venturi, M. *ChemSusChem* **2008**, *1*, 26−58. (c) Imahori, H.; Guldi, D. M.; Tamaki, K.; Yoshida, Y.; Luo, C.; Sakata, Y.; Fukuzumi, S. *J. Am. Chem. Soc.* **2001**, *123*, 6617−6628. (d) Luo, C.; Guldi, D. M.; Imahori, H.; Tamaki, K.; Sakata, Y. *J. Am. Chem. Soc.* **2000**, *122*, 6535−6551. (e) Wasielewski, M. R. *Chem. Rev.* **1992**, *92*, 435−461. (f) Kodis, G.; Liddell, P. A.; de la Garza, L.; Clausen, P. C.; Lindsey, J. S.; Moore, A. L.; Moore, T. A.; Gust, D. *J. Phys. Chem. A* **2002**, *106*, 2036−2048. (g) Kodis, G.; Terazono, Y.; Liddell, P. A.; Andréasson, J.; Garg, V.; Hambourger, M.; Moore, T. A.; Moore, A. L.; Gust, D. *J. Am. Chem. Soc.* **2006**, *128*, 1818−1827. (h) Imahori, H.; Tamaki, K.; Araki, Y.; Sekiguchi, Y.; Ito, O.; Sakata, Y.; Fukuzumi, S. *J. Am. Chem. Soc.* **2002**, *124*, 5165−5174. (i) de la Torre, G.; Giacalone, F.; Segura, J. L.; Martín, N.; Guldi, D. M. *Chem. - Eur. J.* **2005**, *11*, 1267−1280. (j) Giacalone, F.; Segura, J. L.; Martín, N.; Guldi, D. M. *J. Am. Chem. Soc.* **2004**, *126*, 5340−5341. (k) Fujitsuka, M.; Ito, O.; Imahori, H.; Yamada, K.; Yamada, H.; Sakata, Y. *Chem. Lett.* **1999**, *28*, 721−722.

(4) (a) Karlsson, S.; Boixel, J.; Pellegrin, Y.; Blart, E.; Becker, H.-C.; Odobel, F.; Hammarström, L. *Faraday Discuss.* **2012**, *155*, 233−252. (b) Karlsson, S.; Boixel, J.; Pellegrin, Y.; Blart, E.; Becker, H.-C.; Odobel, F.; Hammarström, L. *J. Am. Chem. Soc.* **2010**, *132*, 17977−17979. (c) Pellegrin, Y.; Odobel, F. *Coord. Chem. Rev.* **2011**, *255*, 2578−2593. (d) Hammarström, L. *Acc. Chem. Res.* **2015**, *48*, 840−850.

(5) (a) Lehn, J.-M.; Sauvage, J.-P. *Nouv. J. Chim.* **1977**, *449*, 1−4. (b) Moradpour, A.; Amouyal, E.; Keller, P.; Kagan, H. *Nouv. J. Chim.* **1978**, *2*, 6−12. (c) Kiwi, J.; Gratzel, M. *Nature* **1979**, *281*, 657−658. (d) Kalyanasundaram, K.; Grätzel, M. *Angew. Chem., Int. Ed. Engl.* **1979**, *18*, 701−702. (e) Brown, G. M.; Brunschwig, B. S.; Creutz, C.; Endicott, J. F.; Sutin, N. *J. Am. Chem. Soc.* **1979**, *101*, 1298−1300.

(6) (a) Elvington, M.; Brown, J.; Arachchige, S. M.; Brewer, K. J. *J. Am. Chem. Soc.* **2007**, *129*, 10644−10645. (b) Esswein, A. J.; Nocera, D. G. *Chem. Rev.* **2007**, *107*, 4022−4047. (c) Fihri, A.; Artero, V.; Razavet, M.; Baffert, C.; Leibl, W.; Fontecave, M. *Angew. Chem., Int. Ed.* **2008**, *47*, 564−567. (d) Lazarides, T.; McCormick, T.; Du, P.; Luo, G.; Lindley, B.; Eisenberg, R. *J. Am. Chem. Soc.* **2009**, *131*, 9192−9194. (e) Ozawa, H.; Haga, M.-a.; Sakai, K. *J. Am. Chem. Soc.* **2006**, *128*, 4926−4927. (f) Streich, D.; Astuti, Y.; Orlandi, M.; Schwartz, L.; Lomoth, R.; Hammarström, L.; Ott, S. *Chem. - Eur. J.* **2010**, *16*, 60−63.

(7) (a) Morris, A. J.; Meyer, G. J.; Fujita, E. *Acc. Chem. Res.* **2009**, *42*, 1983−1994. (b) Takeda, H.; Koike, K.; Inoue, H.; Ishitani, O. *J. Am. Chem. Soc.* **2008**, *130*, 2023−2031. (c) Tamaki, Y.; Morimoto, T.; Koike, K.; Ishitani, O. *Proc. Natl. Acad. Sci. U. S. A.* **2012**, *109*, 15673−15678.

(8) Barber, J. *Chem. Soc. Rev.* **2009**, *38*, 185−196.

(9) Kothe, T.; Plumeré, N.; Badura, A.; Nowaczyk, M. M.; Guschin, D. A.; Rögner, M.; Schuhmann, W. *Angew. Chem., Int. Ed.* **2013**, *52*, 14233−14236.

(10) (a) Maeda, K.; Higashi, M.; Lu, D.; Abe, R.; Domen, K. *J. Am. Chem. Soc.* **2010**, *132*, 5858−5868. (b) Sasaki, Y.; Kato, H.; Kudo, A. *J. Am. Chem. Soc.* **2013**, *135*, 5441−5449. (c) Sayama, K.; Mukasa, K.; Abe, R.; Abe, Y.; Arakawa, H. *J. Photochem. Photobiol., A* **2002**, *148*, 71−77.

(11) (a) Kobayashi, R.; Tanigawa, S.; Takashima, T.; Ohtani, B.; Irie, H. *J. Phys. Chem. C* **2014**, *118*, 22450−22456. (b) Sasaki, Y.; Nemoto, H.; Saito, K.; Kudo, A. *J. Phys. Chem. C* **2009**, *113*, 17536−17542. (c) Tada, H.; Mitsui, T.; Kiyonaga, T.; Akita, T.; Tanaka, K. *Nat. Mater.* **2006**, *5*, 782−786. (d) Maeda, K. *ACS Catal.* **2013**, *3*, 1486−

DOI: 10.1021/jacs.5b12650
J. Am. Chem. Soc. 2016, 138, 3752−3760

1503. (e) Zhou, P.; Yu, J.; Jaroniec, M. *Adv. Mater.* **2014**, *26*, 4920−4935.
(12) Sekizawa, K.; Maeda, K.; Domen, K.; Koike, K.; Ishitani, O. *J. Am. Chem. Soc.* **2013**, *135*, 4596−4599.
(13) Andersson, M.; Sinks, L. E.; Hayes, R. T.; Zhao, Y.; Wasielewski, M. R. *Angew. Chem., Int. Ed.* **2003**, *42*, 3139−3143.
(14) (a) Konduri, R.; Ye, H.; MacDonnell, F. M.; Serroni, S.; Campagna, S.; Rajeshwar, K. *Angew. Chem., Int. Ed.* **2002**, *41*, 3185−3187. (b) Gross, M. A.; Reynal, A.; Durrant, J. R.; Reisner, E. *J. Am. Chem. Soc.* **2014**, *136*, 356−366.
(15) Hanna, M. C.; Nozik, A. J. *J. Appl. Phys.* **2006**, *100*, 074510.
(16) Bhosale, S. V.; Jani, C. H.; Langford, S. J. *Chem. Soc. Rev.* **2008**, *37*, 331−342.
(17) Fossum, R. D.; Fox, M. A.; Gelormini, A. M.; Pearson, A. J. *J. Phys. Chem. B* **1997**, *101*, 2526−2532.
(18) Odobel, F.; Zabri, H. *Inorg. Chem.* **2005**, *44*, 5600−5611.
(19) Excitation of the tetrad at 530 nm still excited enough of the Ru unit to observe a long-lived state, but with a lower yield.

DOI: 10.1021/jacs.5b12650
J. Am. Chem. Soc. 2016, 138, 3752−3760